Qualitative Theory of Dynamical Systems (2025) 24:150
https://doi.org/10.1007/s12346-025-01310-1

Novel Superposition Solutions for an Extended (3+1)-Dimensional Generalized Shallow Water Wave Equation in Fluid Mechanics and Plasma Physics

Peng-Fei Han[1] · **Kun Zhu**[1,2] · **Wen-Xiu Ma**[1,3,4,5]

Received: 24 December 2024 / Accepted: 26 May 2025

Abstract

Water waves play a crucial role in elucidating fluid dynamics and plasma physics, as they significantly influence phenomena such as wave propagation, energy transfer, and stability across diverse environments. In this paper, we aim to construct the bilinear auto-Bäcklund transformation and novel function superposition solutions for an extended (3+1)-dimensional generalized shallow water wave equation by employing the Hirota bilinear method and symbolic computation. We meticulously illustrate and analyze the dynamic behavior of interactions between lump waves and two kink waves under various periodic wave backgrounds. This includes the collision of the lump wave with the two kink waves, the splitting of the kink waves, and the emergence and degeneration of the lump wave. By scrutinizing the interactions of breather waves, we observe the fusion and separation phenomena involving bell-shaped waves and breather waves. Additionally, by examining the interactions of rogue waves, we analyze their fission and fusion processes. The interplay among these waves can significantly enhance our understanding of the characteristics of solutions involving function

✉ Wen-Xiu Ma
mawx@cas.usf.edu

Peng-Fei Han
hanpf1995@163.com

Kun Zhu
zhukun@ncnu.edu.cn

1 Department of Mathematics, Zhejiang Normal University, Jinhua 321004, People's Republic of China

2 School of Mathematics and Information Science, Nanchang Normal University, Nanchang 330032, People's Republic of China

3 Department of Mathematics, King Abdulaziz University, Jeddah 21589, Saudi Arabia

4 Department of Mathematics and Statistics, University of South Florida, Tampa 33620-5700, USA

5 Material Science Innovation and Modelling, Department of Mathematical Sciences, North-West University, Mafikeng Campus, Mmabatho 2735, South Africa

Published online: 06 June 2025

superposition, potentially shedding light on certain physical phenomena within the realm of nonlinear science.

Keywords Hirota bilinear method · Lump wave interactions · Bäcklund transformation · Mixed wave interactions

1 Introduction

Extensive research on shallow water wave theory has garnered significant interest in elucidating its formation mechanisms within marine engineering [1–3], ocean dynamics [4–6], and fluid mechanics [7–11]. As a category of nonlinear evolution equations (NLEEs), shallow water wave models have been effectively utilized across various research domains, including applied mathematics [12], hydrodynamics [13], ocean dynamics [14], seawater intrusion [15], and marine engineering [16–18]. Exact solutions play a crucial role in enhancing our comprehension of the intricate physical phenomena and dynamic processes simulated by NLEEs [19–26]. Numerous powerful methods have been developed for this purpose, such as the long wave limit method [27, 28], Darboux transformation [29, 30], Hirota bilinear method [31–35], inverse scattering transform [36, 37], Riemann-Hilbert approach [38], Bäcklund transformation [39], Lie group method [40, 41], and others [42–45].

The application of soliton research in fluid mechanics [46] and plasma physics [47] is of crucial significance. It not only facilitates a deeper understanding of nonlinear wave phenomena within fluids and plasmas but also propels the development of novel theories in applied physics [48]. Solitons, as stable waveforms that emerge in the context of dispersion, dissipation, and diffusion processes, typically arise from the mathematical modeling of physical systems [49]. The soliton solutions derived from these models have garnered considerable interest among researchers [50]. Extensive studies in the literature have explored solitons in conjunction with a broad spectrum of physical phenomena, particularly within the realm of shallow water wave equations [51]. Here, soliton solutions are intricately linked to wave behavior in the actual ocean, which is pivotal for comprehending and forecasting ocean dynamics [52, 53]. These investigations not only enhance our grasp of soliton characteristics but may also uncover certain physical phenomena within the domain of nonlinear science.

Oceanographers confront a diverse array of issues, ranging from the ocean's impact on the Earth's physical climate system to its involvement in the global carbon cycle [54, 55]. The shallow water wave equation is a pivotal tool for these scientists, enabling them to comprehend and anticipate the behavior of ocean waves [56, 57]. This understanding is vital for gaining insights into the impacts of climate change and the intricacies of marine ecosystems [58, 59]. In our research, we will delve into an extended (3+1)-dimensional generalized shallow water wave equation, which is presented as follows:

$$\lambda_1 u_{yt} + \lambda_2 u_{xxxy} + \lambda_3 u_x u_{xy} + \lambda_3 u_{xx} u_y + \lambda_4 u_{xx} + \lambda_5 u_{xy} + \lambda_6 u_{xz} = 0. \quad (1)$$

In the context of oceanographic and atmospheric studies [60], u represents a variable that is dependent on multiple factors, specifically the spatial coordinates x, y, and z, as well as time t, the coefficients λ_1, λ_2, λ_3, λ_4, λ_5 and λ_6 are the real constants. This function u encapsulates the complexity of fluid dynamics within the ocean and atmosphere, where it can denote various physical quantities such as velocity, pressure, or temperature. Several specific instances of Eq. (1) have garnered extensive scholarly attention, particularly those that are integrable models. These integrable models are crucial for understanding wave mechanics and have significant implications in various fields, including fluid dynamics and plasma physics [61–66]:

- By imposing the conditions that u is independent of z and setting the parameters $\lambda_1 = \lambda_2 = 1$, $\lambda_3 = -3$, $\lambda_6 = 0$, Eq. (1) simplifies to the (2+1)-dimensional extended shallow water wave equation as referenced in [61].
- By confining the variable u to not depend on z and assigning the values $\lambda_1 = \lambda_2 = 1$, $\lambda_3 = -3$ and $\lambda_4 = \lambda_5 = \lambda_6 = 0$ to the parameters, Eq. (1) is simplified to the (2+1)-dimensional Boiti-Leon-Manna-Pempinelli equation as documented in reference [62].
- By specifying the parameters $\lambda_1 = \lambda_2 = 1$, $\lambda_3 = -3$, $\lambda_6 = -1$, and setting $\lambda_4 = \lambda_5 = 0$ in Eq. (1), we obtain the (3+1)-dimensional generalized shallow water equation as detailed in [63].
- Assigning the values $\lambda_1 = 2$, $\lambda_2 = 1$, $\lambda_3 = 3$, $\lambda_6 = -3$ and $\lambda_4 = \lambda_5 = 0$ to the parameters in Eq. (1) results in the (3+1)-dimensional Jimbo-Miwa equation as reported in [64–66].

The Hirota bilinear method is recognized as a potent and straightforward approach within the realm of soliton theory [67]. It has been widely applied to NLEEs to construct analytic solutions, demonstrating its effectiveness in various contexts [68–70]. The study of analytic solutions holds significant physical relevance for understanding nonlinear phenomena in shallow water waves, which are crucial for modeling and predicting wave behavior in oceanographic and atmospheric studies [71, 72]. Despite the extensive application of the Hirota bilinear method, there remains a gap in the literature regarding the test function in the form of function superposition. Specifically, research on the superposition of multiple functions to form solutions is relatively limited [73, 74]. Therefore, the purpose of this paper is to explore solutions formed by the superposition of multiple functions, aiming to fill this gap and provide new insights into the behavior of such solutions.

In our research, we focus on the interactions of lump waves with multiple exponential functions and multiple hyperbolic cosine functions. These interactions are particularly intriguing as they can reveal complex wave dynamics that are not evident in simpler models. Additionally, we investigate the interactions between breather waves and rogue waves with other types of waves. This comprehensive study not only explores the mathematical properties of these solutions but also delves into their dynamic characteristics, providing a deeper understanding of the underlying physical phenomena. We have visually depicted the wave interaction phenomena through graphical representations, offering a more intuitive understanding of the complex dynamics involved. This visual approach allows for a clearer interpretation of the solutions and their implications in real-world scenarios.

The progression of the subsequent chapters in this research is described next. In Sect. 2, the Hirota bilinear method is employed to derive the bilinear auto-Bäcklund transformation, lump kink exp-type solutions and lump wave cosh-type solutions of Eq. (1). In Sect. 3, breather wave cos-type solutions and mixed wave cosh-sin-type solutions are constructed using the homoclinic test method. The dynamical behaviors of the wave interactions are illustrated through 3D images. The findings of our study are presented in Sect. 4.

2 Lump Wave Interactions

Within this section, we will utilize the Hirota bilinear method to construct the bilinear auto-Bäcklund transformation and explore the interactions between lump waves and multiple exponential functions. This investigation encompasses both lump kink exp-type solutions and lump wave cosh-type solutions.

2.1 Bäcklund Transformation

To obtain the Hirota bilinear form of Eq. (1), we initiate the derivation by introducing a transformation:

$$u = 6\frac{\lambda_2}{\lambda_3}(\ln f)_x + u_0(z,t). \tag{2}$$

Here, f denotes a function that is differentiable with respect to x, y, z, and t, while $u_0(z,t)$ represents an unspecified function that depends on z and t. Eq. (1) has been reformulated into the subsequent bilinear form:

$$(\lambda_1 D_y D_t + \lambda_2 D_x^3 D_y + \lambda_4 D_x^2 + \lambda_5 D_x D_y + \lambda_6 D_x D_z) f \cdot f = 0, \tag{3}$$

where D_x, D_y, D_z and D_t are the bilinear operators as defined by Hirota [75]. We assume that there exists an additional solution g to the bilinear equation (3):

$$(\lambda_1 D_y D_t + \lambda_2 D_x^3 D_y + \lambda_4 D_x^2 + \lambda_5 D_x D_y + \lambda_6 D_x D_z) g \cdot g = 0. \tag{4}$$

To establish the bilinear auto-Bäcklund transformation between the solutions f and g of the bilinear equation (3), which is associated with Eq. (1), we consider the following form:

$$\begin{aligned} P = {} & [(\lambda_1 D_y D_t + \lambda_2 D_x^3 D_y + \lambda_4 D_x^2 + \lambda_5 D_x D_y + \lambda_6 D_x D_z) f \cdot f] g^2 \\ & - f^2 [(\lambda_1 D_y D_t + \lambda_2 D_x^3 D_y + \lambda_4 D_x^2 + \lambda_5 D_x D_y + \lambda_6 D_x D_z) g \cdot g]. \end{aligned} \tag{5}$$

Given that $P = 0$ in Eq. (5), the function f satisfies the bilinear equation (3) if and only if g satisfies the bilinear equation (4). Consequently, the equations derived under the condition $P = 0$ correspond to the desired bilinear auto-Bäcklund transformations.

By employing the exchange relations for Hirota's bilinear operators [75], we proceed to derive the following results:

$$(D_yD_tf\cdot f)g^2-f^2(D_yD_tg\cdot g)=2D_y(D_tf\cdot g)\cdot(fg)=2D_t(D_yf\cdot g)\cdot(fg), \tag{6a}$$

$$(D_xD_yf\cdot f)g^2-f^2(D_xD_yg\cdot g)=2D_x(D_yf\cdot g)\cdot(fg)=2D_y(D_xf\cdot g)\cdot(fg), \tag{6b}$$

$$(D_xD_zf\cdot f)g^2-f^2(D_xD_zg\cdot g)=2D_x(D_zf\cdot g)\cdot(fg)=2D_z(D_xf\cdot g)\cdot(fg), \tag{6c}$$

$$(D_x^2f\cdot f)g^2-f^2(D_x^2g\cdot g)=2D_x(D_xf\cdot g)\cdot(fg), \tag{6d}$$

and

$$\begin{aligned}&(D_x^3D_yf\cdot f)g^2-f^2(D_x^3D_yg\cdot g)\\&\quad=3D_x[(D_x^2D_yf\cdot g)\cdot(fg)]-D_y[(D_x^3f\cdot g)\cdot(fg)]\\&\qquad+3D_x[(D_yf\cdot g)\cdot(D_x^2f\cdot g)]+3D_y[(D_xf\cdot g)\cdot(D_x^2f\cdot g)].\end{aligned} \tag{7}$$

By substituting Eqs. (6) and (7) into formula (5), Eq. (5) can be transformed into the subsequent form:

$$\begin{aligned}P=\;&3\lambda_2D_y\{(D_xf\cdot g)\cdot[(D_x^2+\rho_1D_x)f\cdot g]\}\\&+3\lambda_2D_x\{(D_yf\cdot g)\cdot[(D_x^2+\rho_2D_y)f\cdot g]\}\\&+D_x\{[(3\lambda_2D_x^2D_y+2\lambda_4D_x+\lambda_5D_y+2\lambda_6D_z)f\cdot g]\cdot(fg)\}\\&+D_y\{[(2\lambda_1D_t-\lambda_2D_x^3+\lambda_5D_x)f\cdot g]\cdot(fg)\},\end{aligned} \tag{8}$$

where ρ_1 and ρ_2 are real constants. Consequently, with $P=0$, the disentanglement of Eq. (8) yields an alternative bilinear auto-Bäcklund transformation for Eq. (1):

$$\begin{aligned}&(D_x^2+\rho_1D_x)f\cdot g=0,\ (2\lambda_1D_t-\lambda_2D_x^3+\lambda_5D_x)f\cdot g=0,\\&(D_x^2+\rho_2D_y)f\cdot g=0,\ (3\lambda_2D_x^2D_y+2\lambda_4D_x+\lambda_5D_y+2\lambda_6D_z)f\cdot g=0.\end{aligned} \tag{9}$$

We choose $f=1$ as a solution for the bilinear form (3) and subsequently solve the bilinear auto-Bäcklund transformation (9) to derive the following equations:

$$\begin{aligned}&g_{xx}+\rho_1g_x=0,\ g_{xx}+\rho_2g_y=0,\\&2\lambda_1g_t-\lambda_2g_{xxx}+\lambda_5g_x=0,\\&3\lambda_2g_{xxy}+2\lambda_4g_x+\lambda_5g_y+2\lambda_6g_z=0.\end{aligned} \tag{10}$$

By assuming $g=1+\exp(v_1x+v_2y+v_3z+v_4t)$ and solving Eq. (10), we derive the relationships among the parameters in the solution g as follows:

$$v_1=-\rho_1,\ v_2=-\frac{\rho_1^2}{\rho_2},\ v_3=\frac{\rho_1(\rho_1\lambda_5+3\rho_1^3\lambda_2+2\rho_2\lambda_4)}{2\rho_2\lambda_6},\ v_4=\frac{\rho_1\lambda_5-\rho_1^3\lambda_2}{2\lambda_1},$$

(11)

where v_1, v_2, v_3 and v_4 are the real constants. Thus, the corresponding exponential function solution for Eq. (1) is

$$u = \frac{6\lambda_2 v_1 \exp(v_1 x + v_2 y + v_3 z + v_4 t)}{\lambda_3[1 + \exp(v_1 x + v_2 y + v_3 z + v_4 t)]} + u_0(z, t), \tag{12}$$

where v_1, v_2, v_3 and v_4 are defined by (11). The example provided above is relatively simple. It is equally plausible to assume alternative forms of g, which could lead to a richer variety of solution types.

2.2 Lump Kink Exp-Type Solutions

To seek the lump kink exp-type solutions for the bilinear form (3), we start by assuming that

$$\begin{aligned} &f_A = a_0 + \eta_1^2 + \eta_2^2 + \sum_{i=1}^{N} h_i \exp(\theta_i),\ \theta_i = \alpha_i x + \beta_i y + \gamma_i z + \omega_i t, \\ &\eta_1 = a_1 x + b_1 y + c_1 z + d_1 t,\ \eta_2 = a_2 x + b_2 y + c_2 z + d_2 t, \end{aligned} \tag{13}$$

where a_0, a_1, b_1, c_1, d_1, a_2, b_2, c_2, d_2, h_i, α_i, β_i, γ_i and ω_i are all the real constants, with N is a positive integer. Furthermore, the resolution of Eq. (1), which includes a quadratic function along with N-exponential functions is provided based on the subsequent Theorem:

Theorem 1 *Supposing that the test function f_A (13) is a solution to Eq. (3) and that one of the four scenarios listed below is satisfied, it follows that the test function f_A (13) indeed solves Eq. (3).*

$$\begin{aligned} &c_1 = \frac{a_2 b_2(\lambda_5 a_1 + \lambda_1 d_1) - \lambda_4 a_1^3}{\lambda_6 a_1^2},\ b_1 = -\frac{a_2 b_2}{a_1},\ d_2 = \frac{a_2 d_1}{a_1}, \\ &\gamma_i = -\frac{\lambda_4 \alpha_i}{\lambda_6},\ \beta_i = 0, \\ &c_2 = -\frac{b_2(\lambda_5 a_1 + \lambda_1 d_1) + \lambda_4 a_1 a_2}{\lambda_6 a_1},\ \omega_i = \frac{d_1 \alpha_i}{a_1} - \frac{\lambda_2 \alpha_i^3}{\lambda_1},\ \lambda_1 \lambda_6 a_1 \neq 0. \end{aligned} \tag{14}$$

$$\begin{aligned} &b_1 = \frac{a_2(\lambda_4 a_2 + \lambda_6 c_2)}{\lambda_1 d_1 + \lambda_5 a_1},\ c_1 = \frac{\lambda_4(a_1^2 + a_2^2) + \lambda_6 a_2 c_2}{-\lambda_6 a_1}, \\ &d_2 = \frac{a_2 d_1}{a_1}, \gamma_i = -\frac{\lambda_4 \alpha_i}{\lambda_6},\ \beta_i = 0, \\ &b_2 = -\frac{a_1(\lambda_4 a_2 + \lambda_6 c_2)}{\lambda_1 d_1 + \lambda_5 a_1}, \omega_i = \frac{d_1 \alpha_i}{a_1} - \frac{\lambda_2 \alpha_i^3}{\lambda_1},\ \lambda_1 \lambda_6 a_1 (\lambda_1 d_1 + \lambda_5 a_1) \neq 0. \end{aligned} \tag{15}$$

$$
\begin{aligned}
&d_1 = -\frac{a_1(\lambda_4 a_1 + \lambda_5 b_1 + \lambda_6 c_1)}{\lambda_1 b_1},\ \omega_i = -\frac{\alpha_i(\lambda_2 b_1 \alpha_i^2 + \lambda_4 a_1 + \lambda_5 b_1 + \lambda_6 c_1)}{\lambda_1 b_1},\\
&b_2 = -\frac{a_1 b_1}{a_2},\ \beta_i = 0,\\
&d_2 = -\frac{a_2(\lambda_4 a_1 + \lambda_5 b_1 + \lambda_6 c_1)}{\lambda_1 b_1},\ c_2 = -\frac{\lambda_4(a_1^2 + a_2^2) + \lambda_6 a_1 c_1}{\lambda_6 a_2},\\
&\gamma_i = -\frac{\lambda_4 \alpha_i}{\lambda_6},\ \lambda_1\lambda_6 a_2 b_1 \neq 0.
\end{aligned}
\tag{16}
$$

$$
\begin{aligned}
&d_1 = \frac{a_1(\lambda_4 a_1^2 - \lambda_5 a_2 b_2 + \lambda_6 a_1 c_1)}{\lambda_1 a_2 b_2},\ \omega_i = \frac{\alpha_i[a_1(\lambda_4 a_1 + \lambda_6 c_1) - a_2 b_2(\lambda_2 \alpha_i^2 + \lambda_5)]}{\lambda_1 a_2 b_2},\\
&b_1 = -\frac{a_2 b_2}{a_1},\\
&d_2 = \frac{a_1(\lambda_4 a_1 + \lambda_6 c_1) - \lambda_5 a_2 b_2}{\lambda_1 b_2},\ c_2 = -\frac{\lambda_4(a_1^2 + a_2^2) + \lambda_6 a_1 c_1}{\lambda_6 a_2},\\
&\gamma_i = -\frac{\lambda_4 \alpha_i}{\lambda_6},\ \beta_i = 0,\ \lambda_1\lambda_6 a_1 a_2 b_2 \neq 0.
\end{aligned}
\tag{17}
$$

Proof of Theorem 1 By the direct computations, substituting the relational expressions (14) and f_A (13) into Eq. (3), it is easy to verify that Eq. (3) is established, then the relational formula f_A (13) is the solution of Eq. (3). Similarly, the other three cases (15), (16) and (17) are also correct. □

Substituting expressions (13) and (14) into transformation (2) to obtain the lump kink exp-type solutions of Eq. (1):

$$
\begin{aligned}
&u_A = 6\frac{\lambda_2}{\lambda_3}(\ln f_A)_x + u_0(z,t),\\
&f_A = a_0 + \eta_1^2 + \eta_2^2 + \sum_{i=1}^{N} h_i \exp\left[\alpha_i x - \frac{\lambda_4 \alpha_i}{\lambda_6} z + \frac{d_1 \alpha_i}{a_1} t - \frac{\lambda_2 \alpha_i^3}{\lambda_1} t\right],\\
&\eta_1 = a_1 x - \frac{a_2 b_2}{a_1} y + \frac{a_2 b_2(\lambda_5 a_1 + \lambda_1 d_1) - \lambda_4 a_1^3}{\lambda_6 a_1^2} z + d_1 t,\\
&\eta_2 = a_2 x + b_2 y - \frac{b_2(\lambda_5 a_1 + \lambda_1 d_1) + \lambda_4 a_1 a_2}{\lambda_6 a_1} z + \frac{a_2 d_1}{a_1} t.
\end{aligned}
\tag{18}
$$

Numerical experiments are conducted to illustrate the characteristics of lump kink exp-type solutions through graphical representations. By setting $N = 2$ in the lump kink exp-type solutions given by Eq. (18), we obtain the solutions that depict the interaction between a lump wave and two kink waves under various background conditions. From Fig. 1, it is evident that the lump wave exhibits a peak and a valley. Their interactions are investigated under various periodic backgrounds. In Fig. 1, panels $(A1)$, $(A2)$ and $(A3)$ explore the interaction between a lump wave and two kink waves in a cosine periodic background. Meanwhile, panels $(B1)$, $(B2)$ and $(B3)$ depict the interaction in the M-type soliton background. As the parameter t increases and the parameter y decreases, the two kink waves and the lump wave propagate along the x-axis and z-axis at a specific angle. One of the kink waves propagates faster than the

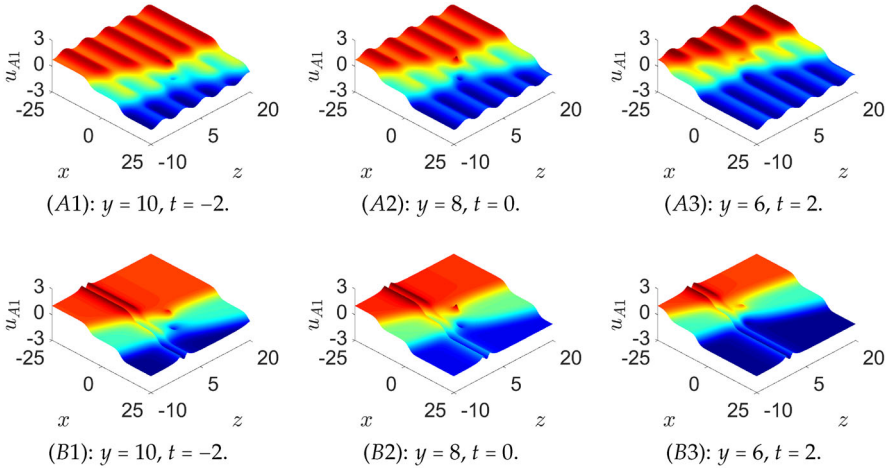

Fig. 1 $(A1)$, $(A2)$, $(A3)$: the interaction between lump wave and two kink waves under the background of cos period via the lump kink exp-type solutions (18) with $u_0(z,t) = \cos(z)/4$. $(B1)$, $(B2)$, $(B3)$: the interaction between lump wave and two kink waves in the M-type soliton background via the lump kink exp-type solutions (18) with $u_0(z,t) = z^2/(z^4+1)$. The profiles are generated by assigning particular values of parameters as $\lambda_1 = \lambda_4 = \lambda_5 = h_1 = h_2 = 1$, $\alpha_1 = \lambda_2 = -1$, $\lambda_3 = 6$, $\lambda_6 = 2$, $a_0 = 0$, $a_1 = 0.6$, $a_2 = 1.5$, $b_2 = -0.8$, $d_1 = 1.4$ and $\alpha_2 = 1.1$

other, eventually overtaking it and resulting in a collision. This collision between the two kink waves induces a change in the amplitude of the lump wave. Following the interaction, the faster kink wave separates from the other due to its higher speed, and the lump wave subsequently recovers its original amplitude.

Investigating the interactions between lump waves and kink waves in different backgrounds is of significant importance for understanding the propagation characteristics of nonlinear waves. In the cosine periodic background, the interactions are primarily characterized by periodic energy transfer and changes in amplitude. In contrast, the interactions in the M-type soliton background are more complex involving changes in the propagation path and energy redistribution. These findings not only enrich the theory of nonlinear waves but also provide theoretical foundations for wave control and energy transfer in practical applications [76, 77]. With the help of expressions (15), (16) and (17), the other three lump kink exp-type solutions of Eq. (1) can be obtained, which will not be introduced one by one here.

2.3 Lump Wave Cosh-Type Solutions

To explore the lump wave cosh-type solutions for Eq. (1), we posit the general solution of the bilinear form (3) in the following manner:

$$\begin{aligned} &f_B = a_0 + \eta_1^2 + \eta_2^2 + \sum_{j=1}^{M} k_j \cosh(\phi_j),\ \phi_j = m_j x + n_j y + p_j z + q_j t, \\ &\eta_1 = a_1 x + b_1 y + c_1 z + d_1 t,\ \eta_2 = a_2 x + b_2 y + c_2 z + d_2 t, \end{aligned} \tag{19}$$

where $a_0, a_1, b_1, c_1, d_1, a_2, b_2, c_2, d_2, k_j, m_j, n_j, p_j, q_j$ are all the real constants, with M is a positive integer.

Theorem 2 *Supposing that the test function f_B (19) is a solution to Eq. (3) and that one of the four scenarios listed below is satisfied, it follows that the test function f_B (19) indeed solves Eq. (3).*

$$\begin{aligned}
&d_1 = -\frac{a_1(\lambda_4 a_2 + \lambda_5 b_2 + \lambda_6 c_2)}{\lambda_1 b_2},\ d_2 = -\frac{a_2(\lambda_4 a_2 + \lambda_5 b_2 + \lambda_6 c_2)}{\lambda_1 b_2},\\
&b_1 = -\frac{a_2 b_2}{a_1},\ p_j = -\frac{\lambda_4 m_j}{\lambda_6},\\
&c_1 = -\frac{\lambda_4(a_1^2 + a_2^2) + \lambda_6 a_2 c_2}{\lambda_6 a_1},\ q_j = -\frac{m_j(\lambda_2 b_2 m_j^2 + \lambda_4 a_2 + \lambda_5 b_2 + \lambda_6 c_2)}{\lambda_1 b_2},\\
&n_j = 0,\ \lambda_1\lambda_6 a_1 b_2 \neq 0.
\end{aligned} \tag{20}$$

$$\begin{aligned}
&c_1 = \frac{b_2(\lambda_5 a_2 + \lambda_1 d_2) - \lambda_4 a_1^2}{\lambda_6 a_1},\ b_1 = -\frac{a_2 b_2}{a_1},\ d_1 = \frac{a_1 d_2}{a_2},\ n_j = 0,\\
&\lambda_1\lambda_6 a_1 a_2 \neq 0,\\
&c_2 = -\frac{b_2(\lambda_5 a_2 + \lambda_1 d_2) + \lambda_4 a_2^2}{\lambda_6 a_2},\ p_j = -\frac{\lambda_4 m_j}{\lambda_6},\ q_j = \frac{d_2 m_j}{a_2} - \frac{\lambda_2 m_i^3}{\lambda_1}.
\end{aligned} \tag{21}$$

$$\begin{aligned}
&b_1 = -\frac{a_1(\lambda_4 a_1 + \lambda_6 c_1)}{\lambda_1 d_1 + \lambda_5 a_1},\ c_2 = -\frac{\lambda_4(a_1^2 + a_2^2) + \lambda_6 a_1 c_1}{\lambda_6 a_2},\\
&d_2 = \frac{a_2 d_1}{a_1},\ p_j = -\frac{\lambda_4 m_j}{\lambda_6},\\
&b_2 = \frac{a_1^2(\lambda_4 a_1 + \lambda_6 c_1)}{a_2(\lambda_1 d_1 + \lambda_5 a_1)},\ q_j = \frac{d_1 m_j}{a_1} - \frac{\lambda_2 m_i^3}{\lambda_1},\ n_j = 0,\\
&\lambda_1\lambda_6 a_1 a_2(\lambda_1 d_1 + \lambda_5 a_1) \neq 0.
\end{aligned} \tag{22}$$

$$\begin{aligned}
&d_1 = \frac{a_2(\lambda_4 a_2 + \lambda_6 c_2) - \lambda_5 a_1 b_1}{\lambda_1 b_1},\ c_1 = -\frac{\lambda_4(a_1^2 + a_2^2) + \lambda_6 a_2 c_2}{\lambda_6 a_1},\\
&b_2 = -\frac{a_1 b_1}{a_2},\ p_j = -\frac{\lambda_4 m_j}{\lambda_6},\ n_j = 0,\\
&d_2 = \frac{a_2^2(\lambda_4 a_2 - \lambda_5 a_1 b_1 + \lambda_6 c_2)}{\lambda_1 a_1 b_1},\ q_j = \frac{m_j[a_2(\lambda_4 a_2 + \lambda_6 c_2) - a_1 b_1(\lambda_2 m_j^2 + \lambda_5)]}{\lambda_1 a_1 b_1},\\
&\lambda_1\lambda_6 a_1 a_2 b_1 \neq 0.
\end{aligned} \tag{23}$$

The proof of Theorem 2 can be similarly referenced to the proof of Theorem 1. Substituting expressions (19) and (20) into transformation (2), the corresponding lump wave cosh-type solutions for Eq. (1) appear as

$$\begin{aligned}
&u_B = 6\frac{\lambda_2}{\lambda_3}(\ln f_B)_x + u_0(z,t),\ f_B = a_0 + \eta_1^2 + \eta_2^2 + \sum_{j=1}^{M} k_j \cosh(\phi_j),\\
&\eta_1 = a_1 x - \frac{a_2 b_2}{a_1} y - \frac{\lambda_4(a_1^2 + a_2^2) + \lambda_6 a_2 c_2}{\lambda_6 a_1} z - \frac{a_1(\lambda_4 a_2 + \lambda_5 b_2 + \lambda_6 c_2)}{\lambda_1 b_2} t,\\
&\eta_2 = a_2 x + b_2 y + c_2 z - \frac{a_2(\lambda_4 a_2 + \lambda_5 b_2 + \lambda_6 c_2)}{\lambda_1 b_2} t,
\end{aligned}$$

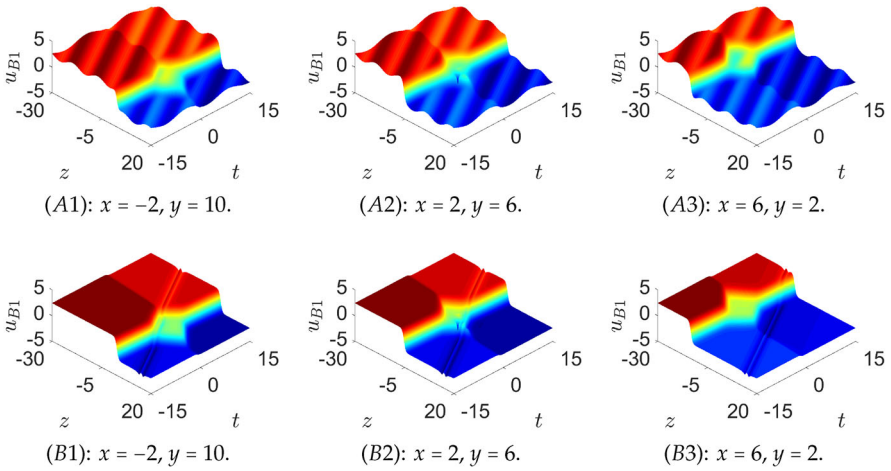

($A1$): $x = -2$, $y = 10$. ($A2$): $x = 2$, $y = 6$. ($A3$): $x = 6$, $y = 2$.

($B1$): $x = -2$, $y = 10$. ($B2$): $x = 2$, $y = 6$. ($B3$): $x = 6$, $y = 2$.

Fig. 2 ($A1$), ($A2$), ($A3$): the interaction between four bending kink waves under the background of sin period via lump wave cosh-type solutions (24) with $u_0(z,t) = 0.5\sin[(z+t)/2]$. ($B1$), ($B2$), ($B3$): the interaction between four bending kink waves in the W-type soliton background via lump wave cosh-type solutions (24) with $u_0(z,t) = -(z+t)^2/[(z+t)^4+1]$. The parameters of ($A1$), ($A2$), ($A3$), ($B1$), ($B2$) and ($B3$) are the same as $\lambda_1 = \lambda_5 = k_1 = k_2 = 1$, $\lambda_2 = \lambda_4 = b_2 = c_2 = -1$, $\lambda_3 = 6$, $\lambda_6 = 2$, $a_0 = 0$, $a_1 = -0.7$, $a_2 = 2$, $m_1 = -2$ and $m_2 = 2.4$

$$\phi_j = m_j x - \frac{\lambda_4 m_j}{\lambda_6} z - \frac{m_j(\lambda_2 b_2 m_j^2 + \lambda_4 a_2 + \lambda_5 b_2 + \lambda_6 c_2)}{\lambda_1 b_2} t. \tag{24}$$

For the lump wave cosh-type solutions given by Eq. (24) with $M = 2$, the three-dimensional dynamic visualizations of these solutions are effectively depicted in Fig. 2. As observed in Fig. 2, four bending kink waves interact with one another under various periodic backgrounds. In Fig. 2, panels ($A1$), ($A2$) and ($A3$) examine the interactions among four bending kink waves against a sine periodic background. Meanwhile, panels ($B1$), ($B2$) and ($B3$) depict the interactions of these four bending kink waves within the W-type soliton background. Fig. 2 illustrates the phenomenon where two kink waves collide and subsequently split into four bending kink waves. These four bending kink waves travel along the negative direction of the z-axis and their interaction results in the formation of a lump wave. Subsequently, the four bending kink waves return to their original state and the lump wave degenerates.

The interactions of four bending kink waves under different backgrounds reveal the rich and complex dynamics of nonlinear wave systems. In the sine periodic background, the interactions are characterized by periodic variations and transient lump wave formation. In contrast, the W-type soliton background provides a more stable environment, leading to enhanced stability and complex interaction patterns. These studies provide valuable insights into the behavior of nonlinear waves in various physical contexts, such as fluid dynamics, plasma physics and optical systems [78, 79].

Using expressions (21), (22) and (23), we can obtain another lump wave cosh-type solutions for Eq. (1). The obtained lump kink exp-type solutions and lump wave cosh-type solutions include the solutions of the studied special equations. When parameters

$\lambda_1 = \lambda_2 = 1, \lambda_4 = \lambda_5 = 0, \lambda_3 = -3, \lambda_6 = -1$ and $N = 1$ in expression (14) are selected, the lump-kink wave solutions [80] and the lumpoff wave solutions [81] of the (3+1)-dimensional generalized shallow water wave equation are obtained. Choosing $M = 1$ in expression (20) can obtain the rouge wave solutions [80, 81] of (3+1)-dimensional generalized shallow water wave equation. When parameters $\lambda_1 = 1$, $\lambda_2 = 3, \lambda_4 = \lambda_6 = 0, \lambda_3 = -3$ and $N = 1$ in expression (14) are selected, the mixed lump-kink solution [82] of the extended shallow water wave model in (2+1)-dimensions is obtained. The lump kink exp-type solutions and lump wave cosh-type solutions not only encompass the solutions of the specific equations under study, but also significantly expand the repertoire of novel solutions for these equations.

3 Mixed Wave Interactions

In this section, we aim to derive the breather wave cos-type solutions and mixed wave cosh-sin-type solutions for Eq. (1). We will explore the interaction between the breather wave and a bell-shaped wave, as well as the interaction of a rogue wave within double bending kink waves.

3.1 Breather Wave Cos-Type Solutions

To derive the breather wave cos-type solutions for the bilinear form (3), we select a test function that comprises an exponential function and cosine functions of the sum type:

$$\begin{aligned} &f_C = r_0 \exp(\eta_3) + \exp(-\eta_3) + \sum_{i=1}^{N} k_i \cos(\theta_i),\ \eta_3 = r_1 x + r_2 y + r_3 z + r_4 t, \\ &\theta_i = \alpha_i x + \beta_i y + \gamma_i z + \omega_i t, \end{aligned} \tag{25}$$

where $r_0, r_1, r_2, r_3, r_4, k_i, \alpha_i, \beta_i, \gamma_i$ and ω_i are real constants, with N is a positive integer.

Theorem 3 *Supposing that the test function f_C (25) is a solution to Eq. (3) and that one of the three scenarios listed below is satisfied, it follows that the test function f_C (25) indeed solves Eq. (3).*

$$\begin{aligned} &r_3 = \frac{\alpha_N \beta_N (\lambda_1 r_4 + 4\lambda_2 r_1^3 + \lambda_5 r_1) - \lambda_4 r_1^3}{\lambda_6 r_1^2},\ \omega_i = \frac{\alpha_i [\lambda_1 r_4 + \lambda_2 r_1 (r_1^2 + \alpha_i^2)]}{\lambda_1 r_1}, \\ &\lambda_1 \lambda_6 r_1 \alpha_i \neq 0, \\ &\gamma_i = \frac{\alpha_N \beta_N [r_1 (3\lambda_2 \alpha_i^2 - \lambda_2 r_1^2 - \lambda_5) - \lambda_1 r_4] - \lambda_4 r_1 \alpha_i^2}{\lambda_6 r_1 \alpha_i}, \\ &r_2 = -\frac{\alpha_N \beta_N}{r_1},\ \beta_i = \frac{\alpha_N \beta_N}{\alpha_i}. \end{aligned} \tag{26}$$

$$
\begin{aligned}
&r_4 = \frac{r_1[r_1(\lambda_4 r_1 + \lambda_6 r_3) - \alpha_N \beta_N (4\lambda_2 r_1^2 + \lambda_5)]}{\lambda_1 \alpha_N \beta_N},\ \beta_i = \frac{\alpha_N \beta_N}{\alpha_i},\ r_2 = -\frac{\alpha_N \beta_N}{r_1},\\
&\quad \lambda_1 \lambda_6 r_1 \alpha_i \beta_N \neq 0,\\
&\gamma_i = \frac{(3\lambda_2 \alpha_N \beta_N - \lambda_4)(r_1^2 + \alpha_i^2) - \lambda_6 r_1 r_3}{\lambda_6 \alpha_i},\\
&\omega_i = \frac{\alpha_i \alpha_N \beta_N [\lambda_2(\alpha_i^2 - 3r_1^2) - \lambda_5] + \alpha_i(\lambda_4 r_1^2 + \lambda_6 r_1 r_3)}{\lambda_1 \alpha_N \beta_N}.
\end{aligned} \tag{27}
$$

$$
\begin{aligned}
&r_3 = \frac{r_2(\lambda_2 \alpha_1^3 - \lambda_1 \omega_1 - \lambda_5 \alpha_1 - 3\lambda_2 r_1^2 \alpha_1) - \lambda_4 r_1 \alpha_1}{\lambda_6 \alpha_1},\\
&\omega_i = \frac{\lambda_1 \omega_1 \alpha_i + \lambda_2 \alpha_1 \alpha_i (\alpha_i^2 - \alpha_1^2)}{\lambda_1 \alpha_1},\\
&\beta_i = -\frac{r_1 r_2}{\alpha_i},\\
&r_4 = \frac{r_1(\lambda_1 \omega_1 - \lambda_2 \alpha_1^3 - \lambda_2 r_1^2 \alpha_1)}{\lambda_1 \alpha_1},\\
&\gamma_i = \frac{r_1 r_2 (\lambda_1 \omega_1 + \lambda_5 \alpha_1 - \lambda_2 \alpha_1^3 - 3\lambda_2 \alpha_1 \alpha_i^2) - \lambda_4 \alpha_1 \alpha_i^2}{\lambda_6 \alpha_1 \alpha_i},\\
&\lambda_1 \lambda_6 \alpha_i \neq 0.
\end{aligned} \tag{28}
$$

The proof of Theorem 3 can be similarly referenced to the proof of Theorem 1. By substituting expressions (26) and (25) into transformation (2), the breather wave cos-type solutions for Eq. (1) are obtained as follows:

$$
\begin{aligned}
&u_C = 6\frac{\lambda_2}{\lambda_3}(\ln f_C)_x + u_0(z,t),\ f_C = r_0 \exp(\eta_3) + \exp(-\eta_3) + \sum_{i=1}^{N} k_i \cos(\theta_i),\\
&\eta_3 = r_1 x - \frac{\alpha_N \beta_N}{r_1} y + \frac{\alpha_N \beta_N (\lambda_1 r_4 + 4\lambda_2 r_1^3 + \lambda_5 r_1) - \lambda_4 r_1^3}{\lambda_6 r_1^2} z + r_4 t,\\
&\theta_i = \alpha_i x + \frac{\alpha_N \beta_N}{\alpha_i} y + \frac{\alpha_N \beta_N [r_1(3\lambda_2 \alpha_i^2 - \lambda_2 r_1^2 - \lambda_5) - \lambda_1 r_4] - \lambda_4 r_1 \alpha_i^2}{\lambda_6 r_1 \alpha_i} z\\
&\qquad + \frac{\alpha_i [\lambda_1 r_4 + \lambda_2 r_1 (r_1^2 + \alpha_i^2)]}{\lambda_1 r_1} t.
\end{aligned} \tag{29}
$$

Let us set $N = 2$ to illustrate the breather wave cos-type solutions in Fig. 3. In Fig. 3, panels $(A1)$, $(A2)$ and $(A3)$ depict the interaction between the breather wave and the bell-shaped wave. As the parameter t increases, the breather wave propagates along the x-axis and z-axis at a specific angle. When the parameter $t = 0$, the bell-shaped wave and the breather wave merge leading to a decrease in the amplitude of the breather wave. Subsequently, the bell-shaped wave and the breather wave gradually separate, and the amplitude of the breather wave recovers. This demonstrates that the interaction between the bell-shaped wave and the breather wave endows the solitary wave with the physical properties of fusion and separation. Panels $(B1)$, $(B2)$ and

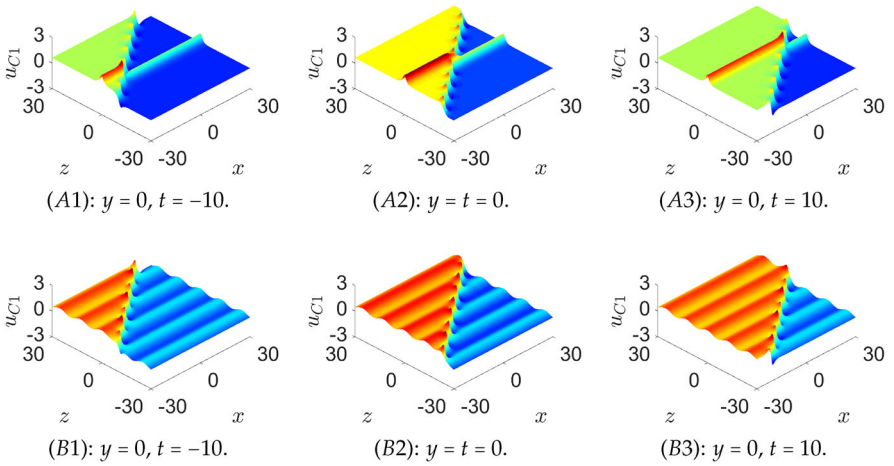

Fig. 3 $(A1), (A2), (A3)$: the interaction between breather wave and bell-shaped wave via breather wave cos-type solutions (29) with $u_0(z,t) = \text{sech}(z)$. $(B1), (B2), (B3)$: the breather wave under the background of cos period via breather wave cos-type solutions (29) with $u_0(z,t) = \cos(z/2)/5$. The profiles are generated by assigning particular values of parameters as $\lambda_1 = \lambda_5 = r_0 = k_1 = r_4 = 1$, $\lambda_2 = \lambda_4 = -1$, $\lambda_3 = 6$, $\lambda_6 = 2$, $k_2 = \alpha_1 = 0.5$, $r_1 = -0.6$, $\alpha_2 = -0.5$ and $\beta_2 = -1.2$

$(B3)$ in Fig. 3 examine the breather wave against a cosine periodic background. Based on expressions (27) and (28), we can derive two additional distinct forms of breather wave cos-type solutions.

The interaction between a breather wave and a bell-shaped wave highlights the dynamic nature of solitary waves, characterized by fusion, separation, and energy transfer. This interaction is crucial for understanding the behavior of nonlinear waves in various physical systems. On the other hand, the breather wave under a cosine periodic background reveals the influence of periodic modulation on wave propagation and stability. These studies provide valuable insights into the complex dynamics of nonlinear waves [83, 84].

3.2 Mixed Wave Cosh-Sin-Type Solutions

Select a trial function that consists of a combination of exponential, hyperbolic cosine and sine functions of the sum type:

$$\begin{aligned} f_D &= r_0 \exp(\eta_3) + \exp(-\eta_3) + \sum_{i=1}^{N} k_i \cosh(\phi_i) + \sum_{j=1}^{M} g_j \sin(\varphi_j), \\ \eta_3 &= r_1 x + r_2 y + r_3 z + r_4 t,\ \phi_i = a_i x + b_i y + c_i z + d_i t, \\ \varphi_j &= m_j x + n_j y + p_j z + q_j t, \end{aligned} \tag{30}$$

where $r_0, r_1, r_2, r_3, r_4, k_i, a_i, b_i, c_i, d_i, g_j, m_j, n_j, p_j$ and q_j are all the real constants to be determined, with N and M are positive integers.

Theorem 4 *Supposing that the test function* f_D (30) *is a solution to Eq.* (3) *and that one of the four scenarios listed below is satisfied, it follows that the test function* f_D (30) *indeed solves Eq.* (3).

$$
\begin{aligned}
c_i &= \frac{(3\lambda_2 m_M n_M - \lambda_4)(a_i^2 - r_1^2) + \lambda_6 r_1 r_3}{\lambda_6 a_i},\\
p_j &= \frac{(3\lambda_2 m_M n_M - \lambda_4)(m_j^2 + r_1^2) - \lambda_6 r_1 r_3}{\lambda_6 m_j},\\
q_j &= \frac{m_j(\lambda_4 r_1^2 + \lambda_6 r_1 r_3) + m_j m_M n_M[\lambda_2(m_j^2 - 3r_1^2) - \lambda_5]}{\lambda_1 m_M n_M},\ r_2 = -\frac{m_M n_M}{r_1},\\
b_i &= -\frac{m_M n_M}{a_i},\\
d_i &= \frac{a_i(\lambda_4 r_1^2 + \lambda_6 r_1 r_3) - a_i m_M n_M[\lambda_2(a_i^2 + 3r_1^2) + \lambda_5]}{\lambda_1 m_M n_M},\ n_j = \frac{m_M n_M}{m_j},\\
r_4 &= \frac{r_1[r_1(\lambda_4 r_1 + \lambda_6 r_3) - m_M n_M(4\lambda_2 r_1^2 + \lambda_5)]}{\lambda_1 m_M n_M},\ \lambda_1\lambda_6 r_1 a_i m_j n_M \neq 0.
\end{aligned}
\tag{31}
$$

$$
\begin{aligned}
r_3 &= \frac{m_M n_M(\lambda_1 r_4 + 4\lambda_2 r_1^3 + \lambda_5 r_1) - \lambda_4 r_1^3}{\lambda_6 r_1^2},\ r_2 = -\frac{m_M n_M}{r_1},\\
b_i &= -\frac{m_M n_M}{a_i},\ \lambda_1\lambda_6 r_1 a_i m_j \neq 0,\\
c_i &= \frac{m_M n_M[r_1(3\lambda_2 a_i^2 + \lambda_2 r_1^2 + \lambda_5) + \lambda_1 r_4] - \lambda_4 r_1 a_i^2}{\lambda_6 r_1 a_i},\ n_j = \frac{m_M n_M}{m_j},\\
d_i &= \frac{a_i[\lambda_1 r_4 + \lambda_2 r_1(r_1^2 - a_i^2)]}{\lambda_1 r_1},\\
p_j &= \frac{m_M n_M[r_1(3\lambda_2 m_j^2 - \lambda_2 r_1^2 - \lambda_5) - \lambda_1 r_4] - \lambda_4 r_1 m_j^2}{\lambda_6 r_1 m_j},\\
q_j &= \frac{m_j[\lambda_1 r_4 + \lambda_2 r_1(r_1^2 + m_j^2)]}{\lambda_1 r_1}.
\end{aligned}
\tag{32}
$$

$$
\begin{aligned}
r_3 &= -\frac{r_2(\lambda_1 d_1 + \lambda_2 a_1^3 + 3\lambda_2 r_1^2 a_1 + \lambda_5 a_1) + \lambda_4 r_1 a_1}{\lambda_6 a_1},\\
d_i &= \frac{\lambda_1 d_1 a_i + \lambda_2 a_1 a_i(a_1^2 - a_i^2)}{\lambda_1 a_1},\ n_j = -\frac{r_1 r_2}{m_j},\\
c_i &= -\frac{r_1 r_2(\lambda_1 d_1 + \lambda_5 a_1 + \lambda_2 a_1^3 + 3\lambda_2 a_1 a_i^2) + \lambda_4 a_1 a_i^2}{\lambda_6 a_1 a_i},\\
q_j &= \frac{\lambda_1 d_1 m_j + \lambda_2 a_1 m_j(a_1^2 + m_j^2)}{\lambda_1 a_1},\ b_i = \frac{r_1 r_2}{a_i},\\
p_j &= \frac{r_1 r_2(\lambda_1 d_1 + \lambda_5 a_1 + \lambda_2 a_1^3 - 3\lambda_2 a_1 m_j^2) - \lambda_4 a_1 m_j^2}{\lambda_6 a_1 m_j},
\end{aligned}
$$

$$r_4 = \frac{r_1(\lambda_1 d_1 + \lambda_2 a_1^3 - \lambda_2 r_1^2 a_1)}{\lambda_1 a_1},\ \lambda_1\lambda_6 a_i m_j \neq 0. \tag{33}$$

$$p_j = \frac{(3\lambda_2 m_M n_M - \lambda_4)(m_j^2 - m_1^2) + \lambda_6 m_1 p_1}{\lambda_6 m_j},$$

$$r_3 = \frac{(3\lambda_2 m_M n_M - \lambda_4)(m_1^2 + r_1^2) - \lambda_6 m_1 p_1}{\lambda_6 r_1},$$

$$d_i = -\frac{a_i m_1(\lambda_4 m_1 + \lambda_6 p_1) + a_i m_M n_M[\lambda_2(a_i^2 - 3m_1^2) + \lambda_5]}{\lambda_1 m_M n_M},\ n_j = \frac{m_M n_M}{m_j},$$

$$r_4 = -\frac{r_1[m_1(\lambda_4 m_1 + \lambda_6 p_1) + m_M n_M(\lambda_2 r_1^2 - 3\lambda_2 m_1^2 + \lambda_5)]}{\lambda_1 m_M n_M},\ r_2 = -\frac{m_M n_M}{r_1},$$

$$q_j = \frac{m_j m_M n_M[\lambda_2(m_j^2 + 3m_1^2) - \lambda_5] - m_1 m_j(\lambda_4 m_1 + \lambda_6 p_1)}{\lambda_1 m_M n_M},\ b_i = -\frac{m_M n_M}{a_i},$$

$$c_i = \frac{(3\lambda_2 m_M n_M - \lambda_4)(a_i^2 + m_1^2) - \lambda_6 m_1 p_1}{\lambda_6 a_i},\ \lambda_1\lambda_6 r_1 a_i m_j n_M \neq 0. \tag{34}$$

The proof of Theorem 4 can be analogously referenced to the proof of Theorem 1. Based on the aforementioned four cases, we can generate different types of mixed wave cosh-sin-type solutions. By substituting expressions (31) and (30) into the transformation (2), the mixed wave cosh-sin-type solutions for Eq. (1) can be expressed as

$$\begin{aligned}
u_D &= 6\frac{\lambda_2}{\lambda_3}(\ln f_D)_x + u_0(z,t),\ f_D = r_0\exp(\eta_3) + \exp(-\eta_3) \\
&\quad + \sum_{i=1}^{N} k_i \cosh(\phi_i) + \sum_{j=1}^{M} g_j \sin(\varphi_j), \\
\eta_3 &= r_1 x - \frac{m_M n_M}{r_1} y + r_3 z + \frac{r_1[r_1(\lambda_4 r_1 + \lambda_6 r_3) - m_M n_M(4\lambda_2 r_1^2 + \lambda_5)]}{\lambda_1 m_M n_M} t, \\
\phi_i &= a_i x - \frac{m_M n_M}{a_i} y + \frac{(3\lambda_2 m_M n_M - \lambda_4)(a_i^2 - r_1^2) + \lambda_6 r_1 r_3}{\lambda_6 a_i} z \\
&\quad + \frac{a_i(\lambda_4 r_1^2 + \lambda_6 r_1 r_3) - a_i m_M n_M[\lambda_2(a_i^2 + 3r_1^2) + \lambda_5]}{\lambda_1 m_M n_M} t, \\
\varphi_j &= m_j x + \frac{m_M n_M}{m_j} y + \frac{(3\lambda_2 m_M n_M - \lambda_4)(m_j^2 + r_1^2) - \lambda_6 r_1 r_3}{\lambda_6 m_j} z \\
&\quad + \frac{m_j(\lambda_4 r_1^2 + \lambda_6 r_1 r_3) + m_j m_M n_M[\lambda_2(m_j^2 - 3r_1^2) - \lambda_5]}{\lambda_1 m_M n_M} t.
\end{aligned} \tag{35}$$

To more clearly elucidate the dynamic behavior of the mixed wave cosh-sin-type solutions, specific parameters are chosen for illustration in the case where $N = M = 1$. In Fig. 4, panels $(A1)$, $(A2)$ and $(A3)$ examine the interaction between a rogue wave and double bending kink waves against a sine periodic background. In Fig. 4, panels $(B1)$,

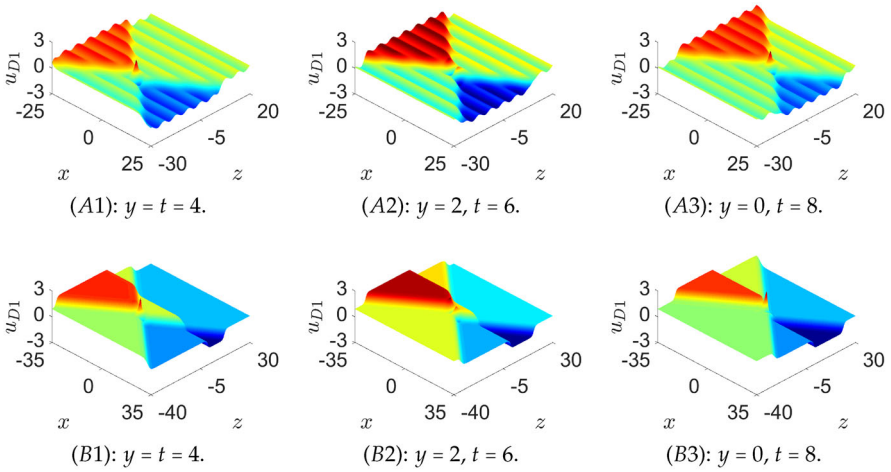

Fig. 4 $(A1)$, $(A2)$, $(A3)$: the interaction between rogue wave and double bending kink waves under the background of sin period via mixed wave cosh-sin-type solutions (35) with $u_0(z,t) = \sin(z)/5$. $(B1)$, $(B2)$, $(B3)$: the interaction between rogue wave and double bending kink waves under a kink wave via mixed wave cosh-sin-type solutions (35) with $u_0(z,t) = \mathrm{sech}[\exp(z)]$. The parameters of $(A1)$, $(A2)$, $(A3)$, $(B1)$, $(B2)$ and $(B3)$ are the same as $\lambda_1 = \lambda_5 = r_0 = 1$, $\lambda_2 = \lambda_4 = -1$, $\lambda_3 = 6$, $\lambda_6 = g_1 = 2$, $k_1 = 0.6$, $r_1 = -0.1$, $r_3 = 1.4$, $a_1 = -1.1$, $m_1 = -1.4$ and $n_1 = -0.3$

$(B2)$ and $(B3)$ simulate the interaction between a rogue wave and double bending kink waves under a kink wave background. Fig. 4 illustrates the interaction between a rogue wave and double bending kink waves. The rogue wave is characterized by an upward peak and a downward valley. As the parameter t increases and y decreases, both the rogue wave and the double bending kink waves propagate in the positive direction along the x-axis and z-axis. Upon collision with the double bending kink waves, the rogue wave splits into two, with a reduction in amplitude. Subsequently, under the influence of the compressive force exerted by the double bending kink waves, the two rogue waves merge back into one, and the amplitude returns to its original level. Throughout this investigation, occurrences of rogue waves undergoing both fission and fusion have been identified.

The interaction between a rogue wave and double bending kink waves under different backgrounds reveals the complex dynamics of nonlinear wave systems. Under a periodic background, the interaction is characterized by periodic modulations and transient changes in wave amplitudes. Under a kink wave background, the interaction is influenced by the structured environment provided by the kink wave, leading to distinct patterns of wave splitting and recombination [85].

Breather wave cos-type solutions (29) and mixed wave cosh-sin-type solutions (35) have been investigated by selecting different parameters and function numbers. Newly observed nonlinear phenomena include the merging and splitting of breather and bell-shaped waves. Additionally, occurrences of rogue waves' division and coalescence have been documented. The physical properties of these solutions are analyzed with the aid of Figs. 3 and 4. Similarly, we can also study the superposition solutions of

more kinds of functions as follows:

$$\begin{aligned} f_E &= \sum_{i=1}^{N} k_i \cosh(\phi_i) + \sum_{j=1}^{M} g_j \sin(\varphi_j) + \sum_{r=1}^{R} h_r \sinh(\theta_r) + \sum_{e=1}^{E} s_e \cos(\eta_e), \\ \phi_i &= a_i x + b_i y + c_i z + d_i t,\ \varphi_j = m_j x + n_j y + p_j z + q_j t, \\ \theta_r &= \alpha_r x + \beta_r y + \gamma_r z + \omega_r t,\ \eta_e = \chi_e x + \varpi_e y + \delta_e z + \tau_e t, \end{aligned} \tag{36}$$

where $k_i, a_i, b_i, c_i, d_i, g_j, m_j, n_j, p_j, q_j, h_r, \alpha_r, \beta_r, \gamma_r, \omega_r, s_e, \chi_e, \varpi_e, \delta_e$ and τ_e are real constants, with N, M, R and E are positive integers. Likewise, the examination of parameter interdependencies can be facilitated through the application of symbolic computation techniques. It is hoped that the superposition solutions (36) can simulate more wave interactions and some new nonlinear phenomena.

4 Discussion and Final Remarks

Based on the Hirota bilinear method and symbolic computation, we have derived the bilinear auto-Bäcklund transformation (9), lump kink exp-type solutions (18), lump wave cosh-type solutions (24), breather wave cos-type solutions (29), and mixed wave cosh-sin-type solutions (35). The construction of these superposition solutions not only encompasses the solutions of the studied special equations but also yields novel superposition solutions for these equations. However, the limitations of this work arise from the fact that the selected functions are not arbitrary elementary functions, such as Jacobian elliptic functions and inverse trigonometric functions. Future work will aim to address these limitations to achieve more extensive results.

Several appropriate examples are provided, and the dynamic analysis of these novel superposition solutions is conducted with the aid of several three-dimensional diagrams. Specifically, Fig. 1 illustrates the variations in the amplitude of the lump wave resulting from the interaction between two kink waves and the lump wave within diverse environmental contexts. Fig. 2 presents the phenomenon of two kink waves splitting, as well as the emergence and decay of the lump wave across various background conditions. Through the selection of suitable parameters, Fig. 3 depicts the coalescence and subsequent separation of the bell-shaped wave and the breather wave under different background conditions. Finally, Fig. 4 shows the interaction of rogue waves in double bending kink waves under different backgrounds.

Shallow water wave equations play a vital role in understanding the dynamics of water waves in rivers, reservoirs, and oceans. They are widely applicable in modeling atmospheric and oceanic flows, as well as in studying wave interactions in various physical contexts [86]. Future research can focus on developing more accurate numerical methods to solve these equations, especially for complex scenarios involving variable bottom topography and non-linear interactions [87]. This is crucial for better predicting and managing coastal and riverine processes, such as tsunamis, storm surges, and river flooding. Additionally, extending the shallow water models to include higher-order corrections can help capture more complex wave behaviors, such as resonant interactions and dispersive shock waves. The study of wave interactions is crucial for

deepening our comprehension of the dynamics inherent in the superposition of functional solutions. Such an analysis not only broadens our theoretical knowledge but also holds the potential to elucidate intricate real-world phenomena that are governed by wave mechanics. By examining how different waves interact and influence each other, we can uncover underlying principles that govern their behavior. This insight is invaluable for developing a more nuanced understanding of wave dynamics, which can be applied to a wide array of scientific and engineering challenges.

Acknowledgements We appreciate the efforts of the reviewers in providing detailed and helpful comments that have contributed to the enhancement of our research. Ma's work was partially supported by the National Natural Science Foundation of China (Grant No. 12271488) and the Ministry of Science and Technology of China (Nos. G2021016032L and G2023016011L). Zhu's work was partially supported by the Natural Science Foundation of Jiangxi Province (Nos. 20224BAB201015 and 20232BAB202034).

Author Contributions Peng-Fei Han, (Conceptualization, Data curation, Formal analysis, Investigation, Software, Supervision, Validation, Writing - original draft, Writing - review and editing)Kun Zhu, (Formal analysis, Software) Wen-Xiu Ma, (Funding acquisition, Methodology, Project administration).

Data Availability All data generated or analyzed during this study are included in this published article.

Declarations

Conflicts of Interest The authors declare that there is no conflict of interests regarding the research effort and the publication of this paper.

References

1. Alam, M.N., Rahman, M.A.: Study of the parametric effect of the wave profiles of the time-space fractional soliton neuron model equation arising in the topic of neuroscience. Partial Differ. Equ. Appl. Math. **12**, 100985 (2024). https://doi.org/10.1016/j.padiff.2024.100985
2. Bekir, A., Aksoy, E.: Exact solutions of extended shallow water wave equations by exp-function method. Int. J. Numer. Method. H. **23**(2), 305–319 (2013). https://doi.org/10.1108/09615531311293489
3. Chen, J.C., Feng, B.F., Chen, Y., Ma, Z.Y.: General bright-dark soliton solution to (2+1)-dimensional multi-component long-wave-short-wave resonance interaction system. Nonlinear Dyn. **88**, 1273–1288 (2017). https://doi.org/10.1007/s11071-016-3309-9
4. Alam, M.N.: An analytical technique to obtain traveling wave solutions to nonlinear models of fractional order. Partial Differ. Equ. Appl. Math. **8**, 100533 (2023). https://doi.org/10.1016/j.padiff.2023.100533
5. Sulaiman, T.A., Yusuf, A., Abdeljabbar, A., Alquran, M.: Dynamics of lump collision phenomena to the (3+1)-dimensional nonlinear evolution equation. J. Geom. Phys. **169**, 104347 (2021). https://doi.org/10.1016/j.geomphys.2021.104347
6. Rao, J.G., He, J.S., Cheng, Y.: The Davey-Stewartson I equation: doubly localized two-dimensional rogue lumps on the background of homoclinic orbits or constant. Lett. Math. Phys. **112**, 75 (2022). https://doi.org/10.1007/s11005-022-01571-w
7. Ma, H.C., Mao, X., Deng, A.P.: Interaction solutions for the second extended (3+1)-dimensional Jimbo-Miwa equation. Chinese Phys. B **32**(6), 060201 (2023). https://doi.org/10.1088/1674-1056/acb91c
8. Wang, K.L.: An efficient scheme for two different types of fractional evolution equations. Fractals **32**(05), 2450093 (2024). https://doi.org/10.1142/S0218348X24500932
9. Ma, Y.L., Li, B.Q.: The dynamics on soliton molecules and soliton bifurcation for an extended generalization of Vakhnenko equation. Qual. Theory Dyn. Syst. **23**(3), 137 (2024). https://doi.org/10.1007/s12346-024-01002-2
10. Wang, D., Gao, Y.T., Yu, X., Deng, G.F., Liu, F.Y.: Painlevé analysis, Bäcklund transformation, Lax pair, periodic-and travelling-wave solutions for a generalized (2+1)-dimensional Hirota-Satsuma-Ito

equation in fluid mechanics. Qual. Theory Dyn. Syst. **23**, 12 (2024). https://doi.org/10.1007/s12346-023-00850-8
11. Gao, X.Y.: In plasma physics and fluid dynamics: Symbolic computation on a (2+1)-dimensional variable-coefficient Sawada-Kotera system. Appl. Math. Lett. **159**, 109262 (2025). https://doi.org/10.1016/j.aml.2024.109262
12. Alam, M.N., Rahim, M.A., Hossain, M.N., Tunç, C.: Dynamics of damped and undamped wave natures of the fractional Kraenkel-Manna-Merle system in ferromagnetic materials. J. Appl. Comput. Mech. **10**(2), 317–329 (2024). https://jacm.scu.ac.ir/article_18685.html
13. Han, P.F., Zhang, Y.: Linear superposition formula of solutions for the extended (3+1)-dimensional shallow water wave equation. Nonlinear Dyn. **109**(2), 1019–1032 (2022). https://doi.org/10.1007/s11071-022-07468-6
14. Alam, M.N., Akash, H.S., Saha, U., Hasan, M.S., Parvin, M.W., Tunç, C.: Bifurcation analysis and solitary wave analysis of the nonlinear fractional soliton neuron model. Iran. J. Sci. **47**(5), 1797–1808 (2023). https://doi.org/10.1007/s40995-023-01555-y
15. Raza, N., Jannat, N., Basendwah, G.A., Bekir, A.: Dynamical analysis and extraction of solitonic structures of a novel model in shallow water waves. Mod. Phys. Lett. B **38**(36), 2450384 (2024). https://doi.org/10.1142/S0217984924503846
16. Ma, Y.L., Li, B.Q.: Soliton interactions, soliton bifurcations and molecules, breather molecules, breather-to-soliton transitions, and conservation laws for a nonlinear (3+1)-dimensional shallow water wave equation. Nonlinear Dyn. **112**(4), 2851–2867 (2024). https://doi.org/10.1007/s11071-023-09185-0
17. Feng, C.H., Tian, B., Gao, X.T.: Bilinear form, *N* solitons, breathers and periodic waves for a (3+1)-dimensional Korteweg-de Vries equation with the time-dependent coefficients in a fluid. Qual. Theory Dyn. Syst. **23**, 291 (2024). https://doi.org/10.1007/s12346-024-01103-y
18. Gao, X.Y.: Hetero-Bäcklund transformation, bilinear forms and multi-solitons for a (2+1)-dimensional generalized modified dispersive water-wave system for the shallow water. Chin. J. Phys. **92**, 1233–1239 (2024). https://doi.org/10.1016/j.cjph.2024.10.004
19. Sun, H.Q., Chen, A.H.: Lump and lump-kink solutions of the (3+1)-dimensional Jimbo-Miwa and two extended Jimbo-Miwa equations. Appl. Math. Lett. **68**, 55–61 (2017). https://doi.org/10.1016/j.aml.2016.12.008
20. Chen, J.C., Yan, Q.X.: Bright soliton solutions to a nonlocal nonlinear Schrödinger equation of reverse-time type. Nonlinear Dyn. **100**, 2807–2816 (2020). https://doi.org/10.1007/s11071-020-05673-9
21. Wang, K.L.: New solitary wave solutions of the fractional modified KdV-Kadomtsev-Petviashvili equation. Fractals **31**(03), 2350025 (2023). https://doi.org/10.1142/S0218348X23500251
22. Rao, J.G., Mihalache, D., Zhou, F., He, J.S., Chen, S.A.: Dark and antidark solitons on continuous and doubly periodic backgrounds in the space-shifted nonlocal nonlinear Schrödinger equation. Chaos Soliton. Fract. **182**, 114846 (2024). https://doi.org/10.1016/j.chaos.2024.114846
23. Li, B.Q., Wazwaz, A.M., Ma, Y.L.: Soliton resonances, soliton molecules to breathers, semi-elastic collisions and soliton bifurcation for a multi-component Maccari system in optical fiber. Opt. Quant. Electron. **56**(4), 573 (2024). https://doi.org/10.1007/s11082-023-06224-3
24. Osman, M.S.: On multi-soliton solutions for the (2+1)-dimensional breaking soliton equation with variable coefficients in a graded-index waveguide. Comput. Math. Appl. **75**, 1–6 (2018). https://doi.org/10.1016/j.camwa.2017.08.033
25. Liu, J.G., Wazwaz, A.M.: Breather wave and lump-type solutions of new (3+1)-dimensional Boiti-Leon-Manna-Pempinelli equation in incompressible fluid. Math. Methods Appl. Sci. **44**, 2200–2208 (2021). https://doi.org/10.1002/mma.6931
26. Giné, J., Sinelshchikov, D.I.: On the geometric and analytical properties of the anharmonic oscillator. Commun. Nonlinear Sci. Numer. Simulat. **131**, 107875 (2024). https://doi.org/10.1016/j.cnsns.2024.107875
27. Han, P.F., Bao, T.: Hybrid localized wave solutions for a generalized Calogero-Bogoyavlenskii-Konopelchenko-Schiff system in a fluid or plasma. Nonlinear Dyn. **108**, 2513–2530 (2022). https://doi.org/10.1007/s11071-022-07327-4
28. Han, P.F., Zhang, Y., Jin, C.H.: Novel evolutionary behaviors of localized wave solutions and bilinear auto-Bäcklund transformations for the generalized (3+1)-dimensional Kadomtsev-Petviashvili equation. Nonlinear Dyn. **111**(9), 8617–8636 (2023). https://doi.org/10.1007/s11071-023-08256-6
29. Ma, Y.L., Li, B.Q.: Phase transitions of lump wave solutions for a (2+1)-dimensional coupled Maccari system. Eur. Phys. J. Plus **139**(1), 93 (2024). https://doi.org/10.1140/epjp/s13360-024-04896-8

30. Ma, W.X.: Binary Darboux transformation of vector nonlocal reverse-time integrable NLS equations. Chaos Soliton. Fract. **180**, 114539 (2024). https://doi.org/10.1016/j.chaos.2024.114539
31. Zhao, H.Q., Ma, W.X.: Mixed lump-kink solutions to the KP equation. Comput. Math. Appl. **74**(6), 1399–1405 (2017). https://doi.org/10.1016/j.camwa.2017.06.034
32. Ma, W.X., Yong, X.L., Zhang, H.Q.: Diversity of interaction solutions to the (2+1)-dimensional Ito equation. Comput. Math. Appl. **75**(1), 289–295 (2018). https://doi.org/10.1016/j.camwa.2017.09.013
33. Ünsal, Ö., Bekir, A., Taşcan, F., Naci Özer, M.: Complexiton solutions for two nonlinear partial differential equations via modification of simplified Hirota method. Wave. Random Complex **27**(1), 117–128 (2017). https://doi.org/10.1080/17455030.2016.1205238
34. Alhami, R., Alquran, M.: Extracted different types of optical lumps and breathers to the new generalized stochastic potential-KdV equation via using the Cole-Hopf transformation and Hirota bilinear method. Opt. Quant. Electron. **54**, 553 (2022). https://doi.org/10.1007/s11082-022-03984-2
35. Ma, H.C., Chen, X.Y., Deng, A.P.: Novel soliton molecule solutions for the second extend (3+1)-dimensional Jimbo-Miwa equation in fluid mechanics. Commun. Theor. Phys. **75**(12), 125004 (2023). https://doi.org/10.1088/1572-9494/ad0960
36. Han, P.F., Ye, R.S., Zhang, Y.: Inverse scattering transform for the coupled Lakshmanan-Porsezian-Daniel equations with non-zero boundary conditions in optical fiber communications. Math. Comput. Simulat. **232**, 483–503 (2025). https://doi.org/10.1016/j.matcom.2025.01.008
37. Han, P.F., Ma, W.X., Ye, R.S., Zhang, Y.: Inverse scattering transform for the defocusing-defocusing coupled Hirota equations with non-zero boundary conditions: Multiple double-pole solutions. Physica D **471**, 134434 (2025). https://doi.org/10.1016/j.physd.2024.134434
38. Zhang, X.F., Tian, S.F., Yang, J.J.: The Riemann-Hilbert approach for the focusing Hirota equation with single and double poles. Anal. Math. Phys. **11**, 86 (2021). https://doi.org/10.1007/s13324-021-00522-3
39. Gao, X.Y.: In the shallow water: Auto-Bäcklund, hetero-Bäcklund and scaling transformations via a (2+1)-dimensional generalized Broer-Kaup system. Qual. Theory Dyn. Syst. **23**(4), 184 (2024). https://doi.org/10.1007/s12346-024-01025-9
40. Jiwari, R., Kumar, V., Singh, S.: Lie group analysis, exact solutions and conservation laws to compressible isentropic Navier-Stokes equation. Eng. Comput-Germany **38**(3), 2027–2036 (2022). https://doi.org/10.1007/s00366-020-01175-9
41. Ma, H.C.: A simple method to generate Lie point symmetry groups of the (3+1)-dimensional Jimbo-Miwa equation. Chinese Phys. Lett. **22**(3), 554 (2005). https://doi.org/10.1088/0256-307X/22/3/010
42. Wang, K.L.: New analysis methods for the coupled fractional nonlinear Hirota equation. Fractals **31**(09), 2350119 (2023). https://doi.org/10.1142/S0218348X23501190
43. Alam, M.N.: Soliton solutions to the electric signals in telegraph lines on the basis of the tunnel diode. Partial Differ. Equ. Appl. Math. **7**, 100491 (2023). https://doi.org/10.1016/j.padiff.2023.100491
44. Zhao, N., Chen, Y.H., Cheng, L., Chen, J.C.: Data-driven soliton solutions and parameter identification of the nonlocal nonlinear Schrödinger equation using the physics-informed neural network algorithm with parameter regularization. Nonlinear Dyn. in press (2024). https://doi.org/10.1007/s11071-024-10562-6
45. Iqbal, M., Alam, M.N., Lu, D.C., Seadawy, A.R., Alsubaie, N.E., Ibrahim, S.: On the exploration of dynamical optical solitons to the modify unstable nonlinear Schrödinger equation arising in optical fibers. Opt. Quant. Electron. **56**(5), 765 (2024). https://doi.org/10.1007/s11082-024-06468-7
46. Han, P.F., Zhang, Y.: Investigation of shallow water waves near the coast or in lake environments via the KdV-Calogero-Bogoyavlenskii-Schiff equation. Chaos Soliton. Fract. **184**, 115008 (2024). https://doi.org/10.1016/j.chaos.2024.115008
47. Yang, X.L., Zhang, Y., Li, W.J.: Dynamics of general soliton and rational solutions in the (3+1)-dimensional nonlocal Mel'nikov equation with non-zero background. Qual. Theory Dyn. Syst. **23**, 211 (2024). https://doi.org/10.1007/s12346-024-01068-y
48. Alam, M.N., Alp İlhan, O., Akash, H.S., Talib, I.: Bifurcation analysis and new exact complex solutions for the nonlinear Schrödinger equations with cubic nonlinearity. Opt. Quant. Electron. **56**(3), 302 (2024). https://doi.org/10.1007/s11082-023-05863-w
49. Yang, J.Y., Ma, W.X.: Abundant interaction solutions of the KP equation. Nonlinear Dyn. **89**, 1539–1544 (2017). https://doi.org/10.1007/s11071-017-3533-y
50. Alam, M.N., Talib, I., Tunç, C.: The new soliton configurations of the 3D fractional model in arising shallow water waves. Int. J. Appl. Comput. Math. **9**(5), 75 (2023). https://doi.org/10.1007/s40819-023-01552-0

51. Gao, X.Y.: Auto-Bäcklund transformation with the solitons and similarity reductions for a generalized nonlinear shallow water wave equation. Qual. Theory Dyn. Syst. **23**(4), 181 (2024). https://doi.org/10.1007/s12346-024-01034-8
52. Cheng, L., Zhang, Y., Ma, W.X., Hu, Y.W.: Wronskian rational solutions to the generalized (2+1)-dimensional Date-Jimbo-Kashiwara-Miwa equation in fluid dynamics. Phys. Fluids. **36**, 017116 (2024). https://doi.org/10.1063/5.0179572
53. Tariq, K.U., Bekir, A., Ilyas, H.: Solitons, lumps, breathers and rouge wave solutions to the (3+1)-dimensional generalized Konopelchenko-Dubrovsky-Kaup-Kupershmidt model. Optik **287**, 171020 (2023). https://doi.org/10.1016/j.ijleo.2023.171020
54. Clarkson, P.A., Mansfield, E.L.: On a shallow water wave equation. Nonlinearity **7**(3), 975 (1994). https://doi.org/10.1088/0951-7715/7/3/012
55. Dullin, H.R., Gottwald, G.A., Holm, D.D.: On asymptotically equivalent shallow water wave equations. Physica D **190**(1–2), 1–14 (2004). https://doi.org/10.1016/j.physd.2003.11.004
56. Thacker, W.C.: Some exact solutions to the nonlinear shallow-water wave equations. J. Fluid Mech. **107**, 499–508 (1981). https://doi.org/10.1017/S0022112081001882
57. Horikis, T.P., Frantzeskakis, D.J., Smyth, N.F.: Extended shallow water wave equations. Wave Motion **112**, 102934 (2022). https://doi.org/10.1016/j.wavemoti.2022.102934
58. Camassa, R., Huang, J.F., Lee, L.: Integral and integrable algorithms for a nonlinear shallow-water wave equation. J. Comput. Phys. **216**(2), 547–572 (2006). https://doi.org/10.1016/j.jcp.2005.12.013
59. Xin, Z.P., Zhang, P.: On the weak solutions to a shallow water equation. Commun. Pur. Appl. Math. **53**(11), 1411–1433 (2000). DOI: https://doi.org/10.1002/1097-0312(200011)53:11<1411::AID-CPA4>3.0.CO;2-5
60. Dullin, H.R., Gottwald, G.A., Holm, D.D.: An integrable shallow water equation with linear and nonlinear dispersion. Phys. Rev. Lett. **87**(19), 194501 (2001). https://doi.org/10.1103/PhysRevLett.87.194501
61. He, L.C., Zhang, J.W., Zhao, Z.L.: *M*-lump and interaction solutions of a (2+1)-dimensional extended shallow water wave equation. Eur. Phys. J. Plus **136**, 192 (2021). https://doi.org/10.1140/epjp/s13360-021-01188-3
62. Tang, Y.N., Zai, W.J.: New periodic-wave solutions for (2+1)- and (3+1)-dimensional Boiti-Leon-Manna-Pempinelli equations. Nonlinear Dyn. **81**, 249–255 (2015). https://doi.org/10.1007/s11071-015-1986-4
63. Liu, J.G., He, Y.: New periodic solitary wave solutions for the (3+1)-dimensional generalized shallow water equation. Nonlinear Dyn. **90**, 363–369 (2017). https://doi.org/10.1007/s11071-017-3667-y
64. Ma, W.X.: Lump-type solutions to the (3+1)-dimensional Jimbo-Miwa equation. Int. J. Nonlinear Sci. Numer. **17**, 355–359 (2016). https://doi.org/10.1515/ijnsns-2015-0050
65. Ma, H.C., Huang, H.Y., Deng, A.P.: Soliton molecules and some interaction solutions for the (3+1)-dimensional Jimbo-Miwa equation. J. Geom. Phys. **170**, 104362 (2021). https://doi.org/10.1016/j.geomphys.2021.104362
66. Ismael, H.F., El-Ganaini, S., Bulut, H.: M-lump waves and their interactions with multi-soliton solutions for the (3+1)-dimensional Jimbo-Miwa equation. Int. J. Nonlin. Sci. Num. **24**(4), 1221–1232 (2023). https://doi.org/10.1515/ijnsns-2021-0468
67. Alquran, M., Alhami, R.: Analysis of lumps, single-stripe, breather-wave, and two-wave solutions to the generalized perturbed-KdV equation by means of Hirota's bilinear method. Nonlinear Dyn. **109**, 1985–1992 (2022). https://doi.org/10.1007/s11071-022-07509-0
68. Gao, X.Y.: Oceanic shallow-water investigations on a generalized Whitham-Broer-Kaup-Boussinesq-Kupershmidt system. Phys. Fluids. **35**, 127106 (2023). https://doi.org/10.1063/5.0170506
69. Liu, J.G., Zhu, W.H., Osman, M.S., Ma, W.X.: An explicit plethora of different classes of interactive lump solutions for an extension form of 3D-Jimbo-Miwa model. Eur. Phys. J. Plus **135**, 412 (2020). https://doi.org/10.1140/epjp/s13360-020-00405-9
70. Wazwaz, A.M., El-Tantawy, S.A.: Solving the (3+1)-dimensional KP-Boussinesq and BKP-Boussinesq equations by the simplified Hirota's method. Nonlinear Dyn. **88**, 3017–3021 (2017). https://doi.org/10.1007/s11071-017-3429-x
71. Shen, Y., Tian, B.: Bilinear auto-Bäcklund transformations and soliton solutions of a (3+1)-dimensional generalized nonlinear evolution equation for the shallow water waves. Appl. Math. Lett. **122**, 107301 (2021). https://doi.org/10.1016/j.aml.2021.107301

72. Gao, X.Y.: Symbolic computation on a (2+1)-dimensional generalized nonlinear evolution system in fluid dynamics, plasma physics, nonlinear optics and quantum mechanics. Qual. Theory Dyn. Syst. **23**(5), 202 (2024). https://doi.org/10.1007/s12346-024-01045-5
73. Ji, Y., Tan, W.: New soliton solutions and trajectory equations of soliton collision to a (2+1)-dimensional shallow water wave model. Qual. Theory Dyn. Syst. **24**(1), 1–24 (2025). https://doi.org/10.1007/s12346-024-01163-0
74. Guo, Y.F., Guo, C.X., Li, D.L.: The lump solutions for the (2+1)-dimensional Nizhnik-Novikov-Veselov equations. Appl. Math. Lett. **121**, 107427 (2021). https://doi.org/10.1016/j.aml.2021.107427
75. Hirota, R.: The Direct Method in Soliton Theory. Cambridge University Press, New York (2004)
76. Rao, J.G., Mihalache, D., He, J.S.: Multiple solitons and breathers on periodic backgrounds in the complex modified Korteweg-de Vries equation. Appl. Math. Lett. **160**, 109308 (2025). https://doi.org/10.1016/j.aml.2024.109308
77. Wang, K.L.: New computational approaches to the fractional coupled nonlinear Helmholtz equation. Eng. Computation. **41**(5), 1285–1300 (2024). https://doi.org/10.1108/EC-08-2023-0501
78. Chen, J.C., Feng, B.F.: Tau-function formulation for bright, dark soliton and breather solutions to the massive Thirring model. Stud. Appl. Math. **150**(1), 35–68 (2023). https://doi.org/10.1111/sapm.12532
79. Ma, H.C., Qi, X.R., Deng, A.P.: Soliton solutions and the interaction behaviour of the (3+1)-dimensional Jimbo-Miwa-like equation. Phys. Scripta **99**(6), 065210 (2024). https://doi.org/10.1088/1402-4896/ad400d
80. Kumar, D., Raju, I., Paul, G.C., Ali, M.E., Haque, M.D.: Characteristics of lump-kink and their fission-fusion interactions, rogue, and breather wave solutions for a (3+1)-dimensional generalized shallow water equation. Int. J. Comput. Math. **99**(4), 714–736 (2022). https://doi.org/10.1080/00207160.2021.1929940
81. Yang, J.J., Tian, S.F., Peng, W.Q., Li, Z.Q., Zhang, T.T.: The lump, lumpoff and rouge wave solutions of a (3+1)-dimensional generalized shallow water wave equation. Mod. Phys. Lett. B **33**(17), 1950190 (2019). https://doi.org/10.1142/S0217984919501902
82. Ismael, H.F., Seadawy, A., Bulut, H.: Multiple soliton, fusion, breather, lump, mixed kink-lump and periodic solutions to the extended shallow water wave model in (2+1)-dimensions. Mod. Phys. Lett. B **35**(8), 2150138 (2021). https://doi.org/10.1142/S0217984921501384
83. Han, P.F., Zhang, Y.: Superposition behavior of the lump solutions and multiple mixed function solutions for the (3+1)-dimensional Sharma-Tasso-Olver-like equation. Eur. Phys. J. Plus **139**(2), 157 (2024). https://doi.org/10.1140/epjp/s13360-024-04953-2
84. Chen, J.C., Yang, B., Feng, B.F.: Rogue waves in the massive Thirring model. Stud. Appl. Math. **151**(3), 1020–1052 (2023). https://doi.org/10.1111/sapm.12619
85. Wang, K.L., Wei, C.F.: Novel optical soliton solutions of the fractional perturbed Schrödinger equation in optical fiber. Fractals in press (2025). https://doi.org/10.1142/S0218348X24501470
86. Alam, M.N., Iqbal, M., Hassan, M., Fayz-Al-Asad, M., Hossain, M.S., Tunç, C.: Bifurcation, phase plane analysis and exact soliton solutions in the nonlinear Schrödinger equation with Atangana's conformable derivative. Chaos Soliton. Fract. **182**, 114724 (2024). https://doi.org/10.1016/j.chaos.2024.114724
87. Mandal, U.K., Das, A., Ma, W.X.: Integrability, breather, rogue wave, lump, lump-multi-stripe, and lump-multi-soliton solutions of a (3+1)-dimensional nonlinear evolution equation. Phys. Fluids. **36**, 037151 (2024). https://doi.org/10.1063/5.0195378